NASA CONTRACTOR REPORT

NASA CR-61202

February 1968

NASA CR-61202

THE MEASUREMENT OF ROCK DEFORMABILITY IN BORE HOLES ON EARTH

ADAPTABILITY TO A LUNAR EXPLORATION PROGRAM

Prepared under Contract No. NSR 05-003-189 by

Richard E. Goodman, Tran K. Van, and Francois E. Heuzé

UNIVERSITY OF CALIFORNIA, BERKELEY

For

NASA-GEORGE C. MARSHALL SPACE FLIGHT CENTER
Huntsville, Alabama

PREFACE

This paper presents the results of one phase of studies conducted during the period March 3, 1967 - February 1, 1968, under NASA research contract NSR-05-003-189, "Materials Studies Related to Lunar Surface Exploration," with the University of California, Berkeley, California.

This research effort is sponsored by the Lunar Exploration Office, NASA Headquarters, and is monitored by the Space Sciences Laboratory, George C. Marshall Space Flight Center.

February 1968 NASA CR-61202

THE MEASUREMENT OF ROCK DEFORMABILITY IN BORE HOLES ON EARTH

ADAPTABILITY TO A LUNAR EXPLORATION PROGRAM

By

Richard E. Goodman, Tran K. Van and
Francoise E. Heuzé

Prepared under Contract No. NSR 05-003-189 by

UNIVERSITY OF CALIFORNIA, BERKELEY

For

Space Sciences Laboratory

NASA-GEORGE C. MARSHALL SPACE FLIGHT CENTER

I N D E X

THE MEASUREMENT OF ROCK DEFORMABILITY IN BORE HOLES

Abstract

Lunar planning of structures founded in or upon rock calls for the determination of mechanical behavior of rock members involved. Testing in bore holes appears to be the most convenient form of investigation.

Devices for measuring rock deformability in bore holes are of three types: dilatometers, which supply an all around radial pressure to the whole of the bore hole wall; bore hole jacks, which supply a unidirectional, self-equilibrating pair of forces to opposed sectors of the wall; and penetrometers, which force a rigid die into a small portion of the wall. These devices are reviewed, and an NX bore hole plate bearing device, a new bore hole jack developed by the authors, is described.

For interpretation of dilatometer data, a simple well-known relation gives E, Young's modulus, in terms of the diametral formation corresponding to each increment of pressure. An expression giving E for bore hole jacks is derived in this paper, and the influence of rock and jack characteristics on data interpretation is analyzed.

Results of bore hole jack tests conducted in earth rocks at three sites showed good agreement with results of other static, in situ loading tests. The results of bore hole jack tests thus definitely reflect the properties of the rock mass rather than of the rock substance. This is because the volume of rock involved in the test, about one cubic foot, is sufficiently large to embrace significant rock defects that are not usually represented in laboratory testing of samples.

The tests are easy to perform and the equipment reasonably light, enabling its adaptation to lunar testing.

THE MEASUREMENT OF ROCK DEFORMABILITY IN BORE HOLES

INTRODUCTION

AAP and post-AAP development of the moon will require consideration of surface and subsurface structures in rock (deep bore holes, scientific stations, underground chambers for storage and waste disposal, etc.). Sound engineering will achieve the optimum results only if based on intimate knowledge of the modes of mechanical behavior of the materials involved. This must be true on the moon as it is on earth. Hence, there is a need for determination of moon rock load-deformation characteristics. These data can also be used in the measurement of in situ stresses in rocks within bore holes. * For mapping and describing various rock members within an earth site, many feet of drill holes are frequently completed. However, quantitative characterization of the rock units on the sole basis of returned samples is apt to be misleading; the softer and weaker components of the rock tend to be lost and the fabric of the rock block - fracture system in situ is not sampled. In contrast, the walls of the borings form virtually complete "samples" of the rock penetrated by the drill.

Accordingly, within the past few years a number of devices have been developed withich can be inserted into a bore hole to apply a load and measure the response directly on its walls. They combine, with respect to other bulkier methods, the advantage of reduced size and deeper investigation.

The following constitutes an extensive view of devices for measuring rock deformability in bore holes on earth. The purpose of this study is to guide appraisal of the adaptability of such measurements to a Lunar Exploration Program.

---

*Heuzé, F. E., and Goodman, R. E., "Techniques for measuring stresses in rock on the earth. Adaptability to a lunar exploration program," Department of Civil Engineering, University of California, Berkeley, February 1968.

BORE HOLE DEFORMABILITY MEASURING INSTRUMENTS

In the last ten to fifteen years a number of testing devices have been constructed which can be inserted into a bore hole to apply a load and measure the direct response of the walls of the bore hole. As summarized in Table 1, these devices are of three types: (1) instruments that supply a uniform internal pressure in the bore hole by pressuring a fluid in an expandable jacket (bore hole dilatometers); (2) devices that supply a unidirectional pressure to a portion of the circumference of the bore hole by forcing apart circular plates (bore hole jacks); and (3) devices that force a small indenting pin into the wall rock (bore hole penetrometers).

Bore Hole Dilatometers

Two types of full circle radial expansion devices have been developed. In the Menard Pressurementer[1, 2], a central measuring cell filled with water is inflated between upper and lower guard cells introduced to minimize end effects. The inflation pressure is obtained from a gas pressure bottle; the bore hole displacement is calculated from the changing diameter during pressuring. The Geoprobe instrument[3] is a somewhat similar device. In the second type of dilatometer, displacements are measured by differential transformers placed across one or more diameters. Instruments of this type known to the authors are the LNEC (Laboratorio Nacionale de Engenharia Civil) device[4], the Janod-Mermin device[5], Come's cell[6], the tube deformeter[7], and the sounding dilatometer[8, 9]. The most elaborate of these is the tube deformeter which has three groups of 8 LVDT's giving the diametral deformation every 60° around the circumference in the center and at each end of the loaded area.

Bore Hole Jacks

To the authors' knowledge, there is presently no dilatometer capable of applying to the rock a pressure greater than 2, 200 psi (see Table I). This is a satisfactory upper limit of pressure for many rock types and exceeds the actual stress level generated by most types of civil engineering works. To reach significant stress levels over a larger volume of rock, it is possible to increase this maximum pressure by driving stiff plates against the bore hole walls by hydraulic pistons, wedges, or flat jacks. In this type of instrument, referred to here as a bore hole jack, a unidirectional, rather than radial, pressure is applied to the rock over two diametrically opposed sectors of the wall 2 β wide (see figure 3a). A disadvantage of bore hole jacks compared to dilatometers is the less precisely known pressure condition under the load; however, there are offsetting advantages. The load being directional, the test can be oriented and focused on certain geologic targets, e. g. it can be used to measure the force necessary to pry apart joint planes intersecting the hole, particularly if visual observation (stratascope, borehole camera) is made before and after jacking. Further, the higher pressures possible allow the test to be carried beyond the elastic region of many rock types allowing an appreciation of strength to be gained. Dilatometers can do this only in weak rocks and soils. As has been noted, a larger volume of rock is affected by the test for a given diameter.

There are 7 bore hole jack devices known to the authors. The Centex cell (central expanding cell)[10, 11] is a split cylindrical sleeve forced apart by the driving of a conical mandrel. It is not always recoverable in deep applications. The German stress strain meter[13] is a similar device in which wedges are spread apart by advancing a screw. Talobre's jack[12] is similar in concept but was designed for use as a stress meter and is limited

to application at shallow depths, i. e., several feet. Panek[14] adapted the flat jack for use in a bore hole, edge welding race track-shaped steel sheets. Intended as a stress meter, the unit must be cemented in the hole for a single measurement; hence it is practical only in special circumstances. The geoextensometer[20] is another bore hole jack employing circular pistons. The contact angle 2 β is about 140° .

Jaeger and Cook[15] suggested the use of four curved jacks manufactured by rolling thin walled tubing about a parallel cylinder. Two diametrically opposed curved jacks could be used to apply a radial pressure over two quadrants while the response of curved jacks in the contiguous quadrants could be used as deformation meters. The theory has been developed but no instrument was actually built and used in the field to the authors' knowledge.

The NX plate bearing device[19*] was developed and first applied by the authors. As shown in Figure 1, it consists of two steel plates with 2 β = 90° forced apart by 12 race track-shaped pistons selected to give maximum hydraulic efficiency. Two LVDT's give the diametral deformation at either end of the 8-inch long plates. Two return pistons close the instrument to a thickness of 2-3/4 inches affording 1/4 inch clearance for positioning in an NX hole. The total piston travel is 1/2 inch; the LVDT's have a linear range of 0.20 inch and are adjusted to begin their linear travel when the plates are about to contact the rock. Ten thousand psi, the maximum pressure in the hydraulic line, produces 9,300 psi unidirectionally against the rock giving a maximum total force of about 158,000 pounds.

---

*Patent Pending - No. 573,920. Inventors: Goodman, Harlemoff, and Horning; licensed by Slope Indicator Co., Seattle, Washington.

Bore Hole Penetrometers

As opposed to jacks and dilatometers which are plane strain devices, bore hole penetrometers are three-dimensional in concept. A small area rigid die is pressed into the bore hole wall. The contact pressure against the rock in these instruments is very high because the area is small. The rock behavior is complex and no theory is presently known to account for it. Interpretation of data is based upon laboratory calibration. The Bureau of Mines boré hole penetrometer[16] is designed to measure rock response to high load at the site of rock bolt anchors. Hult's[17] and Dryselius's[18] devices were designed to function as stiff active gages in stress measurements. Several other stiff stress gages, not described in Table 1, could also be adapted for use as bore hole penetrometers.

INTERPRETATION OF FIELD DATA

The result of deformability testing in a bore hole of diameter d is a curve of applied pressure Q versus diametral deformation u_d. By cycling the load, maintaining the load for extended periods, and using other test procedures common in rock engineering studies, valuable qualitative conclusions can be drawn about the rock properties in addition to quantitative information. If the Poisson's ratio of the rock (ν) is assumed or measured, a bore hole dilatometer or jack gives an expression for Young's modulus from the ratio of ΔQ to $\Delta u_d/d$ for each load increment as discussed below. The selection of final values of deformation modulus for design purpose, as for other in situ tests, will make use of engineering judgement based in part on results obtained from all tests performed in a comprehensive testing program. An example of this is given in Table 5.

Table 1

DEVICES FOR MEASURING ROCK DEFORMABILITY IN BOREHOLES

TYPE	PRESSURE CONDITION	INTERPRETATION FORMULA	NAME OF DEVICE	METHOD OF PRESSURE APPLICATION	METHOD OF MEASURING DEFORMATION	NUMBER OF DIAMETERS MEASURED	DIAMETER OF BOREHOLE (MM) (INCHES)	LENGTH OF LOADED AREA (MM) (INCHES)	MAX. CONTACT PRESSURE (PSI)	CAN IT BE RECOVERED AFTER USE?	COUNTRY OF ORIGIN	REFERENCES	REMARKS
DILATOMETERS	UNIFORM RADIAL PRESSURE ALL AROUND THE CIRCUMFERENCE OF THE BOREHOLE	$E = \frac{\Delta p}{\Delta(U_d/d)}(1+\nu)$	MENARD PRESSUREMETER	GAS PRESSURE AGAINST WATER FILLING CELL	VOLUME CHANGE ON EXPANSION	INTEGRATED EFFECT OF ALL DIAMETERS	76 3.0 60 2 3/8 48 2.0 32 1 1/2	515 19 1/2 502 19 686 26 910 34 1/2	1500	YES	FRANCE	1,2	CONSIDERABLE EXPERIENCE RECORD
			GEOPROBE INSTRUMENT	DITTO	DITTO	DITTO	76 3.0	?	1500	YES	?	3	
			L.N.E.C. DEVICE	PUMP OIL TO EXPAND CELL	4 LVDTs	4	76 3.0	540 21.2	2200	YES	PORTUGAL	4	
			JANOD-MERMIN DEVICE	DITTO	3 LVDTs	3	168 6.6	770 30.4	2200	YES	FRANCE	5	
			COMES' CELL	DITTO	3 LVDTs	3	160 6.3	1600 63.0	2200	YES	FRANCE	6	
			TUBE DEFORMETER	DITTO	24 LVDTs	4	297 11.7	1300 51.2	660	YES	JAPAN	7	
			SOUNDING DILATOMETER	DITTO	2 "MCH" INSTRUMENTS	2	200 7.9 300 11.8	1000 39.3 1200 47.2	600 1000	YES	YUGOSLAVIA	8,9	
BOREHOLE JACKS	UNIDIRECTIONAL FORCE OF 2 STIFF PLATES EACH CONTACTING ROCK OVER AN ANGLE 2β	$E = \frac{\Delta p}{\Delta(U_d/d)} K_1(\nu,\beta)$	N X PLATE BEARING TEST	PUMP OIL TO DRIVE PISTONS	2 LVDTs	1	76 3.0	204 8.0	9300	YES	USA	19, AND THIS ARTICLE	$2\beta = 90°$
			CENTEX CELL (CEBTP DEVICE)	PUMP OIL TO DRIVE A CONICAL MANDREL INTO A SPLIT CYLINDER	DISTANCE MANDREL IS DRIVEN MEASURED INDUCTIVELY	1	76 3.0	306 12.0	?	NOT ALWAYS IN DEEP HOLES	FRANCE	10, 11	$2\beta \approx 140°$
			GEOEXTENSOMETER (NEW CEBTP DEVICE)	PUMP OIL TO DRIVE PISTONS	2 LVDTs	1	76 3.0	306 12	5000?	YES	FRANCE	20	$2\beta = 143°$
			TALOBRE'S JACK	PUMP OIL TO DRIVE PISTONS	?	1?	56 2.2	≈120 4.7	?	YES	FRANCE	12	2β BELIEVED TO BE ABOUT 90°, INTENDED AS STRESS METER; LIMITED TO SHALLOW DEPTH
			GERMAN STRESS STRAIN METER	SPREAD WEDGES BY DRIVING A SCREW	"NO CONTACT" INDUCTION PICK UP	1	50 2.0	63 2.5	HIGH	NOT ALWAYS	GERMANY	13	SLIGHTLY <180°
			PANEK'S BOREHOLE FLAT JACK	PUMP OIL INTO A FLAT JACK CEMENTED IN THE BOREHOLE	NOT DONE AT PRESENT; COULD BE MEASURED BY GAGING ACROSS INSIDE OF FLAT JACK	1	CAN BE TAILOR-MADE FOR ANY LENGTH AND DIAMETER		3-4000	NO	USA	14	2β SLIGHTLY <180°. INTENDED AS STRESS METER; COULD BE ADAPTED BUT SEVERE EDGE EFFECTS
	RADIAL PRESSURE OVER OPPOSED 2β SECTORS	$E = \frac{\Delta p}{\Delta(U_d/d)} K_2(\nu,\beta)$	QUADRANTAL JACKS	PUMP OIL INTO CURVED JACKS IN OPPOSED QUADRANTS	RESPONSE OF PASSIVE JACKS IN OTHER TWO QUADRANTS	INTEGRATED EFFECT OF ALL DIAMETERS	DITTO		3-4000	YES	AUSTRALIA AND SOUTH AFRICA	15	$2\beta = 90°$; TEST NEVER ACTUALLY PERFORMED IN SITU. COULD BE ADAPTED FOR SHALLOW APPLICATIONS
BOREHOLE PENETROMETERS	UNIDIRECTIONAL PRESSURE OVER A SMALL AREA	EMPIRICAL RELATIONSHIP	BUREAU OF MINES PENETROMETER	PUMP OIL TO DRIVE PISTON FORCING INDENTING PIN	DIAL GAGE EXTENSOMETER WITH CABLE DRIVE	1	32 1.25	9.5 3/8	VERY HIGH	YES	USA	16	3/8" DIAM INDENTING PIN FORCED INTO WALL; DESIGNED TO MEASURE ROOF BOLT ANCHORAGE CAPABILITY; LIMITED DEPTH
			HULT'S DEVICE	PUMP OIL TO DRIVE PISTON DEFORMING PROVING RING	STRAIN GAGES ON PROVING RING	1	32 1.25	≈3 1/8	VERY HIGH	YES	SWEDEN	17	CA 1/8" SQUARE PIECE FORCED INTO WALL BY DEFORMATION OF PROVING RING. DESIGNED AS ACTIVE STIFF GAGE FOR STRESS MEASUREMENTS
			DRYSELIUS' DEVICE (CTH 3)	PUMP OIL TO DRIVE 3 PISTONS AT 60°	STRAIN GAGES ON CANTILEVER ELEMENTS	3	44	≈5 ≈0.2	VERY HIGH	YES	SWEDEN	18	3 PINS FORCED INTO WALL BY OIL PISTONS. DESIGNED AS ACTIVE STIFF GAGE

U_d = DIAMETRAL DISPLACEMENT, d = DIAMETER OF BOREHOLE, p = APPLIED PRESSURE

FIGURE 1a NX BOREHOLE PLATE BEARING TEST DEVICE.

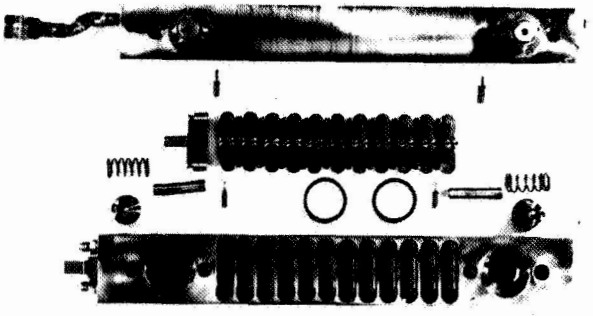

FIGURE 1b DEVICE DISASSEMBLED.

Bore Hole Dilatometer Data

An expression for E is easily derived from the thick walled cylinder formulas[25] by solving for the displacements under internal pressure Q when the outer radius goes to infinity and the outer pressure is zero. This gives:

$$E = \frac{\Delta Q}{u_d/d}(1 + \nu) \qquad (1)$$

Even if the rock mass is under initial stress, this approach is still valid unless the rock is highly nonlinear as the displacements on pressuring the dialtometer are due only to the applied load. E will be computed as a tangent modulus along the (ΔQ, $\Delta \nu$) curve (see figure 9). As in any loading test, the lowest values for E are generally obtained at the lowest stress levels and the highest along the linear portion of the load deformation curve at the highest stress level when no fracture or yielding takes place.

Bore Hole Jack Data

Quantitative interpretation of measurements made with bore holejacks involves a more difficult formula because the loading is not continuous over the circumference of the bore hole wall. Further, except in the case of Jaeger and Cook's Quadrantal curved jacks[15], the force is directed at an inclination to the normal to the bore hole wall at all points except the line of symmetry. The boundary condition to be satisfied is one of constant displacement rather than constant pressure. The steel plates are much stiffer than the rock and will be driven out with very little bending. The boundary pressure will not be uniform and pressure readings will represent an average value over the steel-rock boundary. However, as will be shown, constant displacement solutions are very little different from constant pressure

solutions in this class of problems if the average pressure and average displacement over the plate - rock contact area are used in computations.

(a) Radial Pressure Over Diametrically Opposed Sectors of the Bore Hole Wall

The solution to this problem was obtained by Jaeger and Cook[15] using the complex variable method. The complete derivation is given in the Appendix. The radial displacement (u_r) at an angular distance from the center line of the plate, where the plate extends from $+\beta$ to $-\beta$ (figure 3a) is given by

$$\frac{\pi E}{(1+\nu)} \frac{u_r}{a Q} = -2\beta - \sum_{n=1}^{\infty} \frac{1}{n} \left(\frac{3-4\nu}{2n-1} + \frac{1}{2n+1} \right) \cos 2n\theta \sin 2n\beta \qquad (2)$$

The average displacement of plates of given angle 2β may be obtained by integration. The resulting formula for E would only apply in the case of jacks with radial applied pressure; as yet there are none. This formula should not be used to interpret uniaxially acting bore hole jacks.

(b) Unidirectional Pressure Over Diametrically Opposed Sectors of the Bore Hole Wall

This is theoretically the problem posed by the use of uniaxially acting bore hole jacks. A unidirectional constant pressure boundary condition from $-\beta$ to $+\beta$ may be resolved into a constant radial boundary pressure over the borehole section of width 2β, and shear and radial pressures distributed sinusoidally over the width 2β as depicted in the Appendix. In the course of this investigation, a solution was obtained for the sinusoidally varying shear and normal force on the wall (Appendix). Superposition with Jaeger's solution (Eq. 2) yields the following formula for the radial displacement

of a point on the wall at 0 from the line of symmetry.

$$\frac{\pi E}{1+\nu}\frac{u_r}{a Q} = 2\beta\left[1 + (3-4\nu)\cos 2\theta\right] + \sum_{m=1}^{\infty}\frac{1}{m}\sin 2m\beta$$

$$\left[\frac{(3-4\nu)}{2m+1}\cos 2(m+1)\theta + \frac{(3-4\nu)}{2m-1}\cos 2m\theta\right.$$

$$\left. + \frac{1}{2m+1}\cos 2m\theta + \frac{1}{2m-1}\cos 2(m-1)\theta\right] \qquad (3)$$

The average displacement is found by integrating the horizontal displacement over the vertical component of each arc segment in contact with the plate, i. e. from $-\beta$ to $+\beta$. The result, shown fully in Eq. 31, Appendix, may be written

$$E = \frac{\Delta Q}{\Delta \bar{u}_d/d} K(\nu, \beta) \qquad (4)$$

where $\Delta\bar{u}_d$ is the average diametral displacement for a given increment of pressure ΔQ and d is the bore hole diameter. Values of $K(\nu, \beta)$ are given in Table 2.

BORE HOLE JACK TEST - DISCUSSION OF DATA INTERPRETATION

Influence of Plate Width

Figure 2a, plotted from Table 2, shows the variation of K with change in β, the angle subtended by half the plate width of arc. The quantity K, according to Eq. 4, is the slope of the line relating E to the ratio of the measured quantities ΔQ and $\Delta u_d/d$. The variation of K with β thus affords a comparison of the sensitivity of jacks designed for different plate widths. The maximum sensitivity -- the highest value of K -- occurs at values of β about 45° (figure 2a), the width selected in designing the NX plate bearing

TABLE 2

Values of K (ν, β) for Use in Equation 4 -- Analytical Solution

β	ν: 0	0.05	0.10	0.15	0.20	0.25	0.30	0.35	0.40	0.45	0.50
5.0	0.434	0.433	0.430	0.424	0.417	0.407	0.396	0.382	0.366	0.348	0.327
10.0	0.704	0.703	0.698	0.690	0.678	0.663	0.645	0.622	0.597	0.568	0.536
15.0	0.904	0.903	0.897	0.887	0.873	0.854	0.831	0.803	0.772	0.735	0.694
20.0	1.052	1.051	1.046	1.035	1.019	0.998	0.973	0.942	0.906	0.864	0.818
25.0	1.159	1.159	1.154	1.143	1.127	1.105	1.078	1.045	1.007	0.963	0.914
30.0	1.230	1.231	1.227	1.217	1.201	1.179	1.152	1.119	1.080	1.035	0.985
35.0	1.271	1.274	1.271	1.262	1.247	1.226	1.200	1.168	1.129	1.086	1.036
40.0	1.287	1.291	1.290	1.282	1.269	1.250	1.225	1.195	1.159	1.117	1.069
45.0	1.282	1.288	1.288	1.282	1.271	1.254	1.232	1.204	1.170	1.131	1.087
50.0	1.261	1.268	1.270	1.266	1.257	1.243	1.224	1.199	1.169	1.133	1.092
55.0	1.227	1.236	1.240	1.238	1.232	1.221	1.204	1.183	1.156	1.125	1.088
60.0	1.186	1.197	1.202	1.203	1.199	1.190	1.177	1.160	1.137	1.109	1.077
65.0	1.142	1.154	1.161	1.164	1.162	1.156	1.146	1.132	1.113	1.089	1.062
70.0	1.098	1.111	1.120	1.124	1.125	1.122	1.114	1.103	1.088	1.068	1.045
75.0	1.059	1.073	1.083	1.089	1.091	1.090	1.085	1.076	1.064	1.048	1.028
80.0	1.028	1.042	1.053	1.061	1.064	1.065	1.061	1.055	1.044	1.031	1.013
85.0	1.007	1.022	1.034	1.042	1.046	1.048	1.046	1.040	1.031	1.019	1.004
90.0	1.000	1.015	1.027	1.035	1.040	1.042	1.040	1.035	1.027	1.015	1.000

test device. It should be noted here that for small values of β, corresponding to narrow plates, a punching failure of the rock might take place. However, this would hardly be the case when β is as large as 45° .

Effect of Poisson's Ratio

Figure 2b shows that for a given ΔQ and $\Delta u_d/d$, the interpretation of E is fairly insensitive to Poisson's ratio (ν), except at high values of ν. A 50% overestimation in ν, from 0.2 to 0.3, would lead to a 3.25% underestimate of E. If ν were taken as 0.4 rather than the assumed true value of 0.2, and error of 100%, the value assigned for E would be underestimated by 8.50% As opposed to E, ν is not subject to large discrepancies between field and laboratory values. Thus simple testing on cores retrieved from the bore hole would give a value representative enough to preclude such large errors on the Poisson's ratio, hence reducing the error on E to a negligible amount.

Effect of Non Linear Rock Properties

Qualitative interpretation of bore hole jack or dilatometer data in rock exhibiting non linear stress - strain behavior is entirely appropriate and meaningful. However, as the entire analytical discussion assumes linear elastic relations, quantitative interpretation using these results, even in incremental form, may be erroneous.

Effect of Steel Plate

The mathematical solution to the bore hole jack problem was derived for a condition of constant horizontal pressure on the inner boundary. In actual fact the boundary condition on the loaded border of the bore hole is complex and unknown owing to the unknown coupling between the steel plates and the rock surface. Figure 3a presents a reasonable charcterization of the

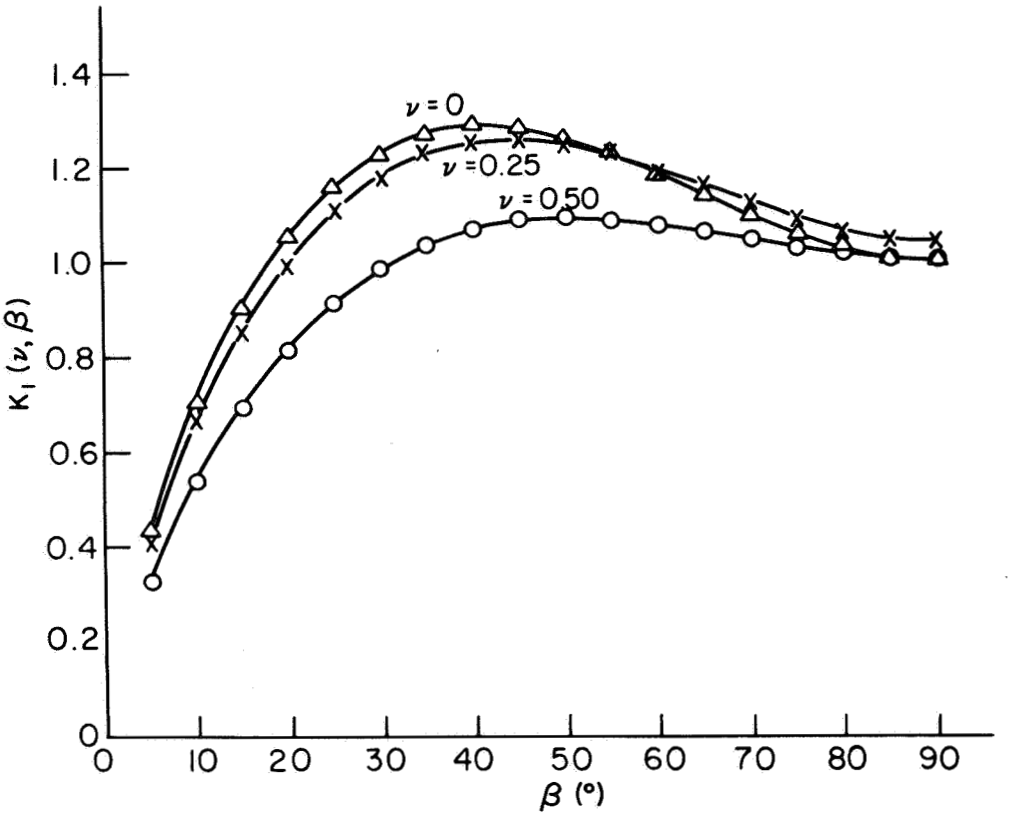

FIGURE 2a. VARIATION OF $K(\nu,\beta)$ WITH RESPECT TO β.

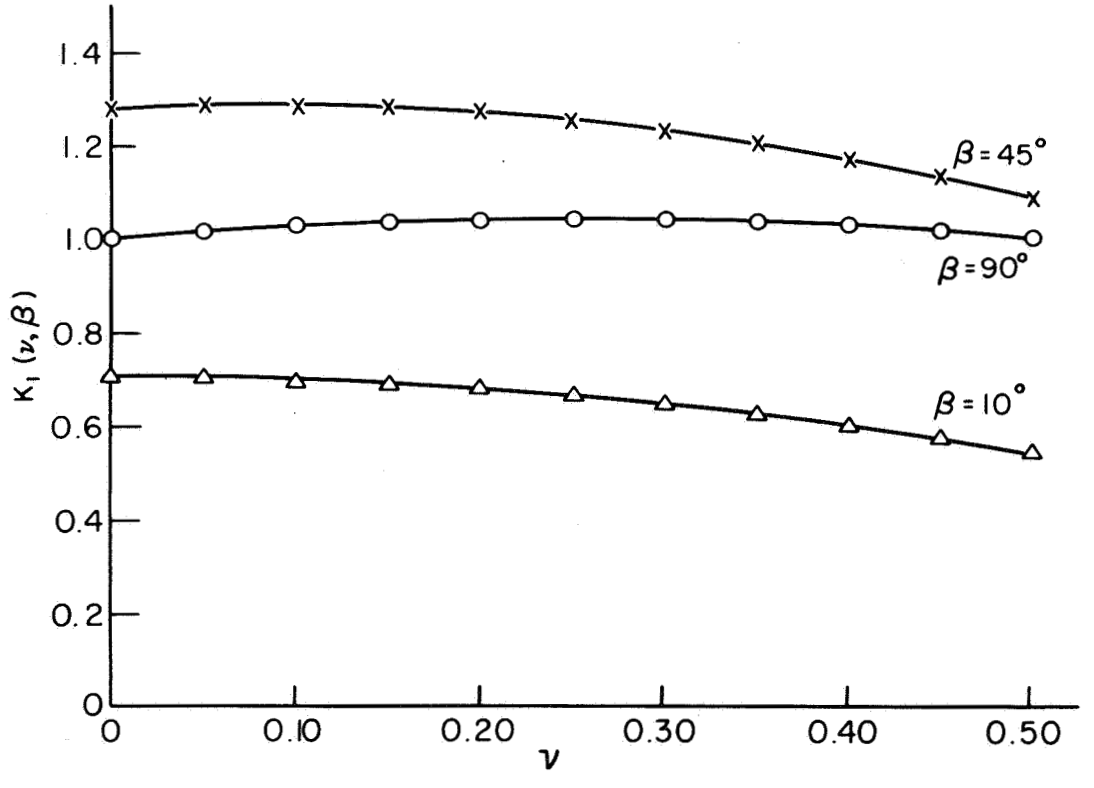

FIGURE 2b. VARIATION OF $K(\nu,\beta)$ WITH RESPECT TO POISSON'S RATIO (ν).

actual boundary condition in the bore hole plate bearing device. A uniform hydraulic pressure bears against the inner sides of the plates. Except in very hard rock, the plates are so much stiffer than the rock as to be driven outward with little bending. The result is a nearly constant horizontal displacement of the rock border; other components of displacement may be considered to exist and be unequal according to the friction and Poisson's ratio contrast between the steel and the rock.

To assess the significance of this departure from the assumed boundary condition, constant displacement and constant pressure solutions were compared for $\nu = 0.25$ using the method of finite element analysis in plane strain. A fine mesh was used with 775 nodal points and 720 elements. The pressure distribution and displacement vectors along the wall of the bore hole are compared for the constant pressure and constant displacement solutions, in figures 3b, c and 3d, e, respectively.

The procedure consists of inputing a constant pressure (or constant X displacement) along the boundary jack-bore hole, computing the average X displacement (or pressure) from the output, and using the average value obtained in Eq. 1. For $\beta = 45°$ and $\nu = 0.25$, one obtains $K = 1.250$ for the constant X displacement case and $K = 1.235$ for the constant pressure case as compared to $K = 1.254$ for the exact analytical solutions. The constant X displacement case is believed to be the more representative of actual field behavior and its simulation by finite element analysis gave the closest result to exact solutions ($K = 1.250$ versus $K = 1.254$). This is the extent of the finite element approximation.

Effect of Finite Test Length

The plane strain solution assumes an infinite test length. In actual fact the NX bore hole plate bearing device has a length to diameter ratio of

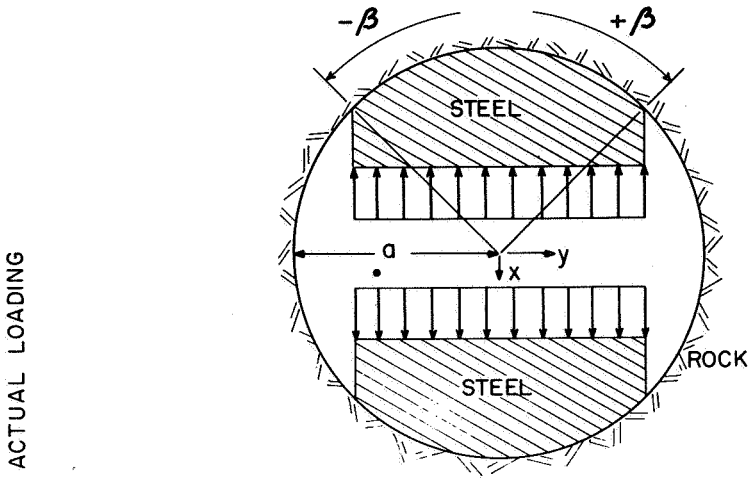

3a. ACTUAL BOUNDARY CONDITION.

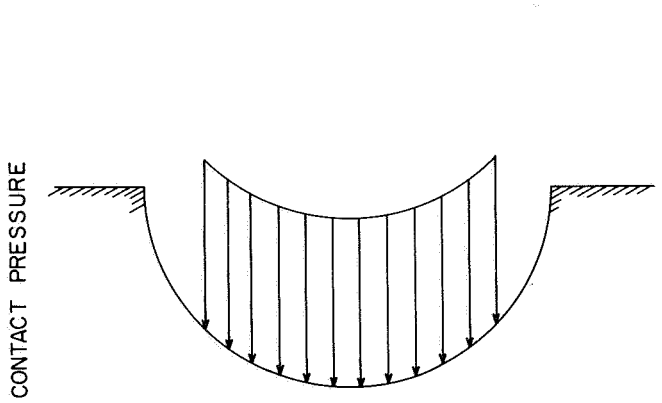

3b. CONSTANT PRESSURE = 10,000 PSI.

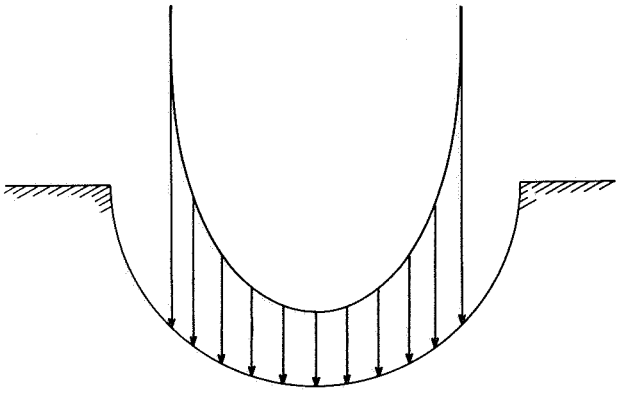

3d. CONTACT PRESSURE RESULTING FROM 3e.

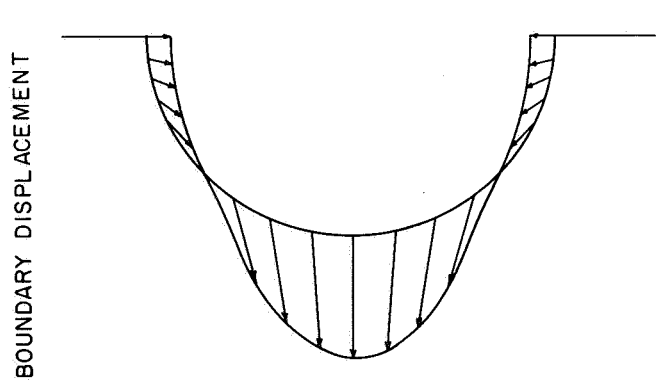

3c. CONTACT DISPLACEMENT RESULTING FROM 3b.

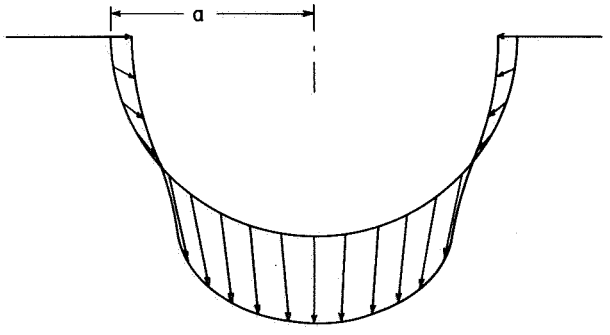

3e. CONSTANT DISPLACEMENT $U_x = 0.01a$.

FIGURE 3. COMPARISON OF CONSTANT PRESSURE AND CONSTANT DISPLACEMENT SOLUTIONS WITH PLANE STRAIN REPRESENTATION OF JACK PROBLEM.

$E = 1.0 \times 10^6$ PSI

$\nu = 0.25$

SCALE OF DISPLACEMENT

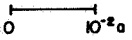

SCALE OF PRESSURE

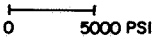

8"/3". To calculate the effect of the finite plate is a difficult three dimensional problem in prismatic space which could not be solved in closed form.* However, an estimate of the end effect was obtained by performing a three dimensional finite element analysis using a new computer program developed by Professor E. L. Wilson[26]. In this approach, a load of finite length is applied to a portion of a longer space whose cross section is constant. The variation of load along the length of the space is achieved by Fourier expansion making repeated cumulative passes through the problem.

Figure 4 gives the variation of displacement at the border of the bore hole over the width and length subjected to uniform pressure ($\nu = 0.25$). The value of K corresponding to the average displacement under the loaded area is 1.06. The corresponding value from finite element analysis of the plane strain approximation is 1.23. Thus the finite length may be taken into account by reducing by 14% values of E derived from Eq. 4 and Table 2, i. e.

$$E = 0.86\, K(\nu)\, \frac{\Delta Q}{\Delta u_d / d} \tag{5}$$

In the NX bore hole plate bearing device, d = 3 inches, and Q is 93% of the hydraulic pressure Q_h. Putting these values in Eq. 5 yields the following equation for interpretation of field data in tests with this instrument.

$$E = 2.40\, K(\nu)\, \frac{\Delta Q_h}{\Delta u_d} \tag{6}$$

*The related three dimensional problem of a hydrostatic pressure of finite length 2 c in a circular hole of radius a was solved by tranter in 1946 (Qtly of Applied Mathematics, vol. 4, p. 298). The three dimensional effect was 37% for c/a = 0.5 and was decreasing rapidly with increased load length. In the NX plate bearing test, c/a = 2.67.

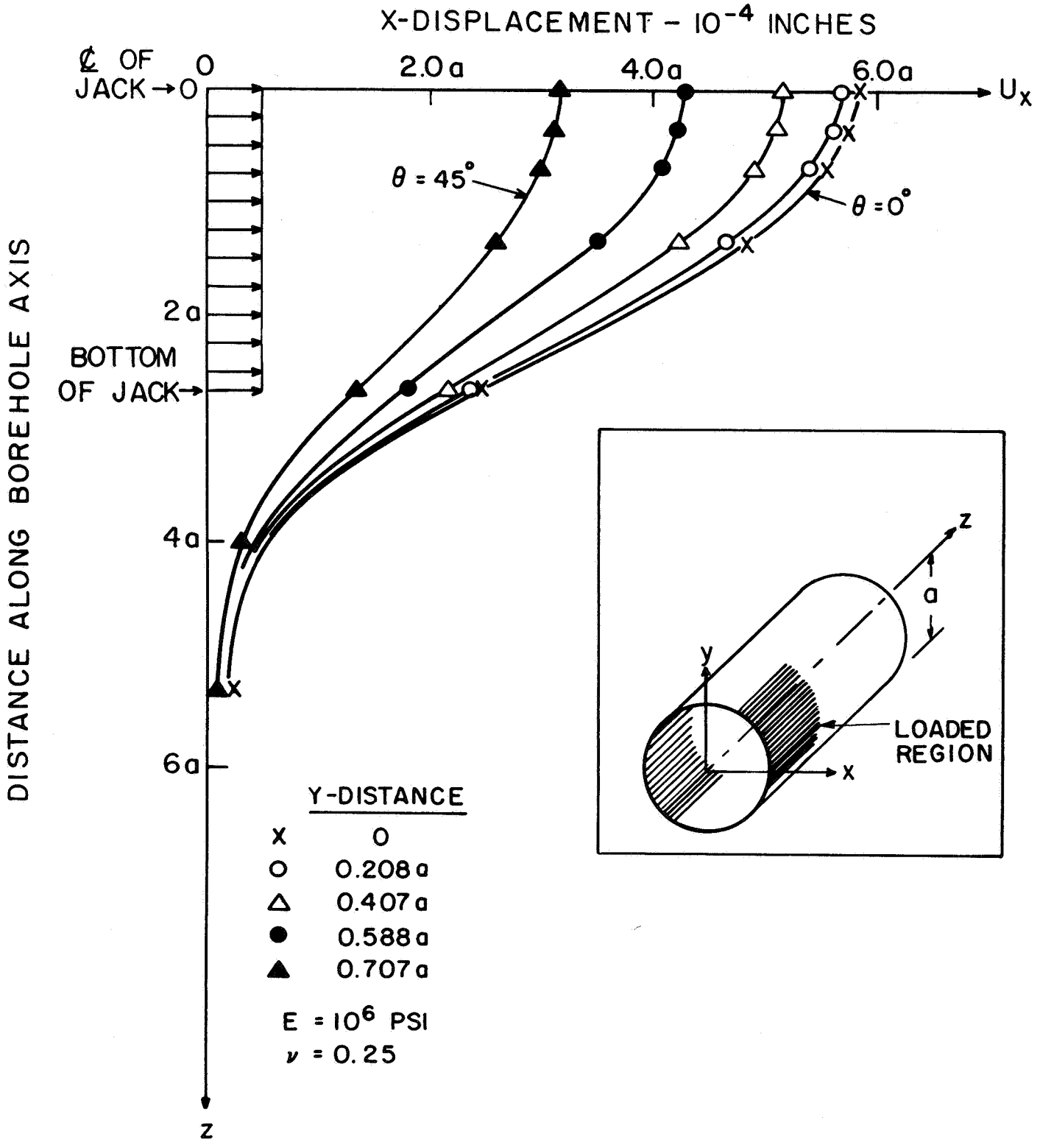

FIGURE 4. VARIATION OF X-DISPLACEMENT ALONG THE BOREHOLE (z DIRECTION) AT DIFFERENT POINTS AROUND THE WALL OF THE BOREHOLE. PRISMATIC-SPACE - CONSTANT PRESSURE = 375 PSI.

TABLE 3

Values of Constants in Equation 6

ν	0	0.05	0.10	0.15	0.20	0.25	0.30	0.35	0.40	0.45	0.50
K (ν)	1.38	1.29	1.29	1.28	1.27	1.25	1.23	1.20	1.17	1.13	1.09
2.40 K (ν)	3.07	3.10	3.10	3.07	3.05	3.00	2.95	2.88	2.81	2.71	2.62

Rock Stress with the Bore Hole Jack

The complex variable method leads to series formulas for the stress components in the rock, as presented in the Appendix. The thrusting apart of the bore hole by the action of the jack leads to a tangential tension on the wall of the bore hole at $\theta = 90°$.

$$\sigma_\theta = -4\beta \frac{Q}{\pi}$$

For the NX bore hole plate bearing device, $\beta = \pi/4$ giving a tangential stress concentration at $\theta = 90°$ of - 1.0. The onset of tensile cracking at this point could be used as a measure of the tensile strength of the rock if a bore hole camera is used concurrently. From Eq. 32, one also obtains at $\theta = 0°$, $\sigma_\theta = 0.875\,Q$ (compressive).

The stresses around the bore hole expressed as a concentration of the jack pressure are presented in figures 5a, b, and c.

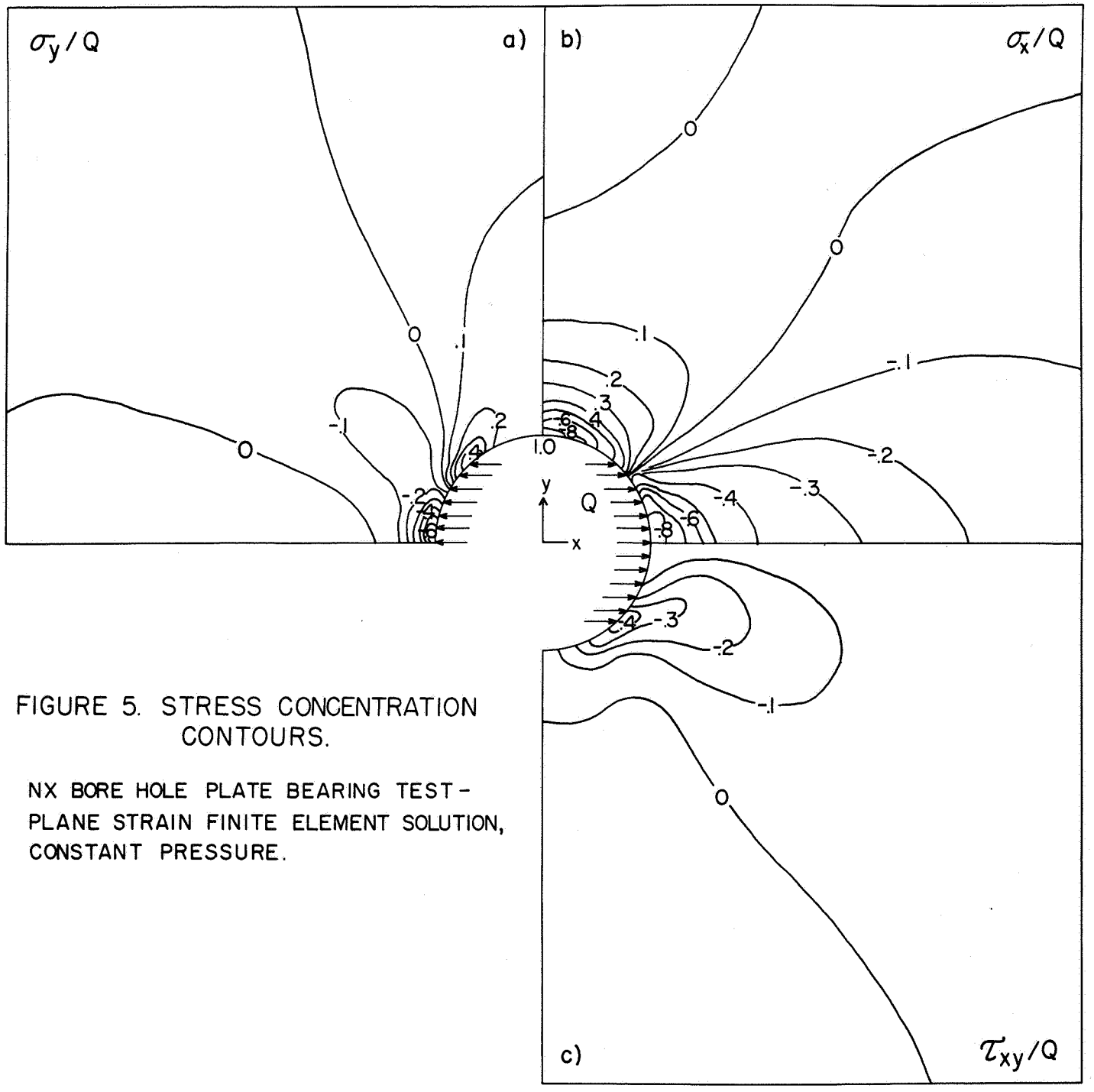

FIGURE 5. STRESS CONCENTRATION CONTOURS.

NX BORE HOLE PLATE BEARING TEST - PLANE STRAIN FINITE ELEMENT SOLUTION, CONSTANT PRESSURE.

Influence of Possible Crack Formation

In all that precedes, the rock has been assumed to be homogeneous, isotropic and linearly elastic. Moreover, no failure criterion has been considered around the bore hole. However, owing to the magnitude of stresses which the jack can induce, superimposed onto the in situ stress concentrations, it is not unlikely that cracking might develop around the bore hole particularly in soft or weak rocks. Cracks could be originated and propagated primarily in those regions where high tensile stresses are found to develop; the critical ones will be the tangential stresses. Then, upon data analysis, corrections shall be introduced to take care of the apparent reduction in the computed modulus of ealsticity to obtain the true value for intact rock. Both concepts presented above are now discussed.

The complete tangential stress field at selected points (on the walls of the bore hole and in the planes of principal stresses) around the bore hole can be readily obtained by superposition of the effects of in situ biaxial stress field (S, T) and of jacking (Q). Figure 6a gives the tangential stress concentration factors. Depending upon the ratio S/T, the stress pattern before jack pressurization can take different forms. They are shown on Figure 6b assuming that $S/T = N = \nu/(1 - \nu)$ (lateral constraint). If S and T have been actually measured, the proper value will then be used. Upon application of a jack pressure Q, the additional tangential stress induced is for $\beta = 45°$ at $\theta = 90°$, $\sigma_\theta = -Q$ and at $\theta = 0°$, $\sigma_\theta = 0.875\,Q$. Accordingly, the complete tangential stress pattern at the selected points is shown on Figures 6c and 6d when jacking takes place in the direction of either principal stress. These are the two extreme cases in terms of tangential stress magnitude. It can be seen that the most unfavorable situation is when jacking takes place in the direction of the minor principal stress. High tensile tangential stresses will then be induced in the plane perpendicular to the direction of jacking,

and the lower the Poisson's ratio of the rock, the higher their magnitude.

In the eventuality of crack formation in a plane perpendicular to the direction of jacking, the observed displacement of the jack plates will be greater than the one taking place in an intact body. Thus, the modulus of elasticity computed from load - deformation curves will be lower than if no crack is initiated. Evaluation of the required correction on E was attempted by simulation technique. The constant X displacement finite element model was used according to previous conclusions. Cracking was simulated by allowing no tensile strength for a certain distance d from the bore hole along the plane perpendicular to the direction of jacking. Three cases were considered:

d = a/2 (crack extending to a half radius distance)

d = a (crack extending to a one radius distance)

d = 5a (simulates a half infinite medium for all practical purposes)

The results are compared in Table 4 with the case of no cracking.

TABLE 4

Influence of Possible Crack Formation

Length of Crack	K	Variation in K	Apparent Decrease in E
0	1.250	+ 0	---
a/2	1.410	+ 13%	- 13%
a	1.553	+ 24%	- 24%
5 a	1.614	+ 29%	- 29%

Unless indicated by a break, or yield point, in the load deformation curve, cracking a depth in a borehole would be monitored by means of bore hole camera, but its extent from the wall inside would be extremely difficult to mea sure. However, from figure 5b, one can see that at a distance, d = 1 radius, the maximum tensile tangential stress induced by jacking has decreased to 0.1 Q (maxiumum value = 930 psi). Moreover, within a short distance from

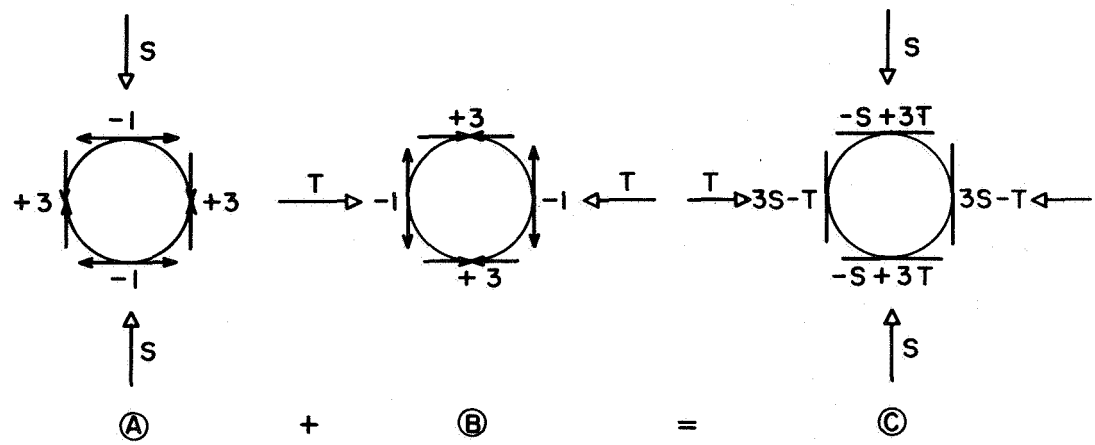

a) TANGENTIAL STRESS CONCENTRATION FACTORS AROUND A BOREHOLE IN A BIAXIAL STRESS FIELD.

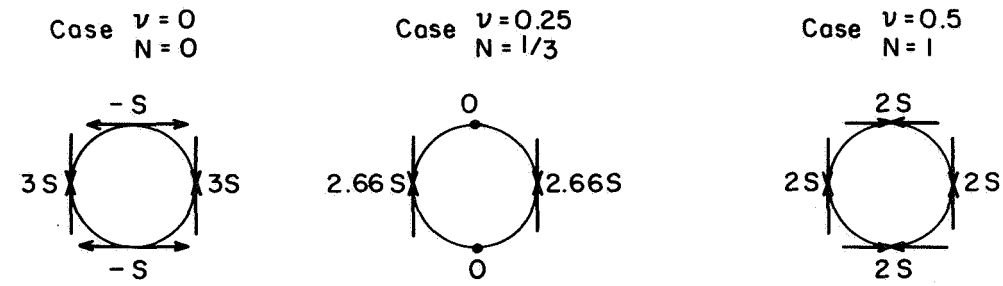

b) TANGENTIAL STRESSES AROUND BOREHOLE — NO JACKING.

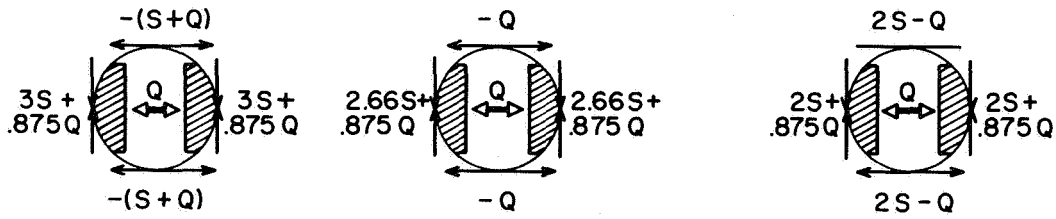

c) JACKING IN DIRECTION OF MINOR PRINCIPAL STRESS.

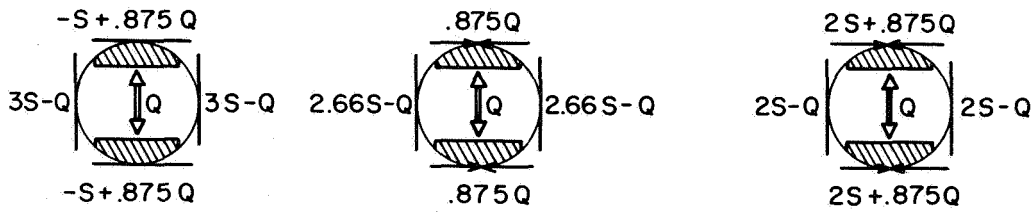

d) JACKING IN DIRECTION OF MAJOR PRINCIPAL STRESS.

S = MAJOR PRINCIPAL STRESS (positive in compression)
T = MINOR PRINCIPAL STRESS (positive in compression)
Q = JACK PRESSURE (positive)

FIGURE 6.

the bore hole, the in situ stress field is again compressive. Thus it is very unlikely that a crack could propagate beyond between 1/2 and 1 radius from the bore hole even in the weakest rock. Accordingly, the corresponding maximum correction to be introduced in the computed modulus of elasticity will probably never exceed 15%. This is well within the limits of accuracy required for engineering purposes knowing that usually results of any test are checked against results obtained by other methods. In case of jacking across a joint intersecting the borehole, the required correction could reach close to 30% and it is suggested that a close examination of jacking explacements be made before actual testing in order to avoid the influence of major discontinuities in the rock mass.

Influence of Wall Roughness and Roundness

Other investigators[30, 31] have analyzed the influence of borehole wall roughness and roundness on the accuracy of stress determinations from borehole deformations. They conclude that with modern diamond drilling equipment and honing devices the morphology of the bore holes enable accurate measurements. In the case of jack testing, crushing of asperities might take place at the beginning of loading but the modulus of deformation is obtained from the linear portion of the load deformation curve which corresponds to a uniform loading. After Suzuki[30], roughness can be limited to about 10^{-3} inches, whereas, plate displacement is of the order of several 10^{-2} inches, so that for practical purposes, no correction will have to be introduced.

The Size of Bore Hole Jack Tests

A bore hole jack produces non homogeneous stress and displacement fields in the rock around the bore hole. Figures 5a, b, and c give the rate at which the applied pressure decays with depth, and figure 7 presents the

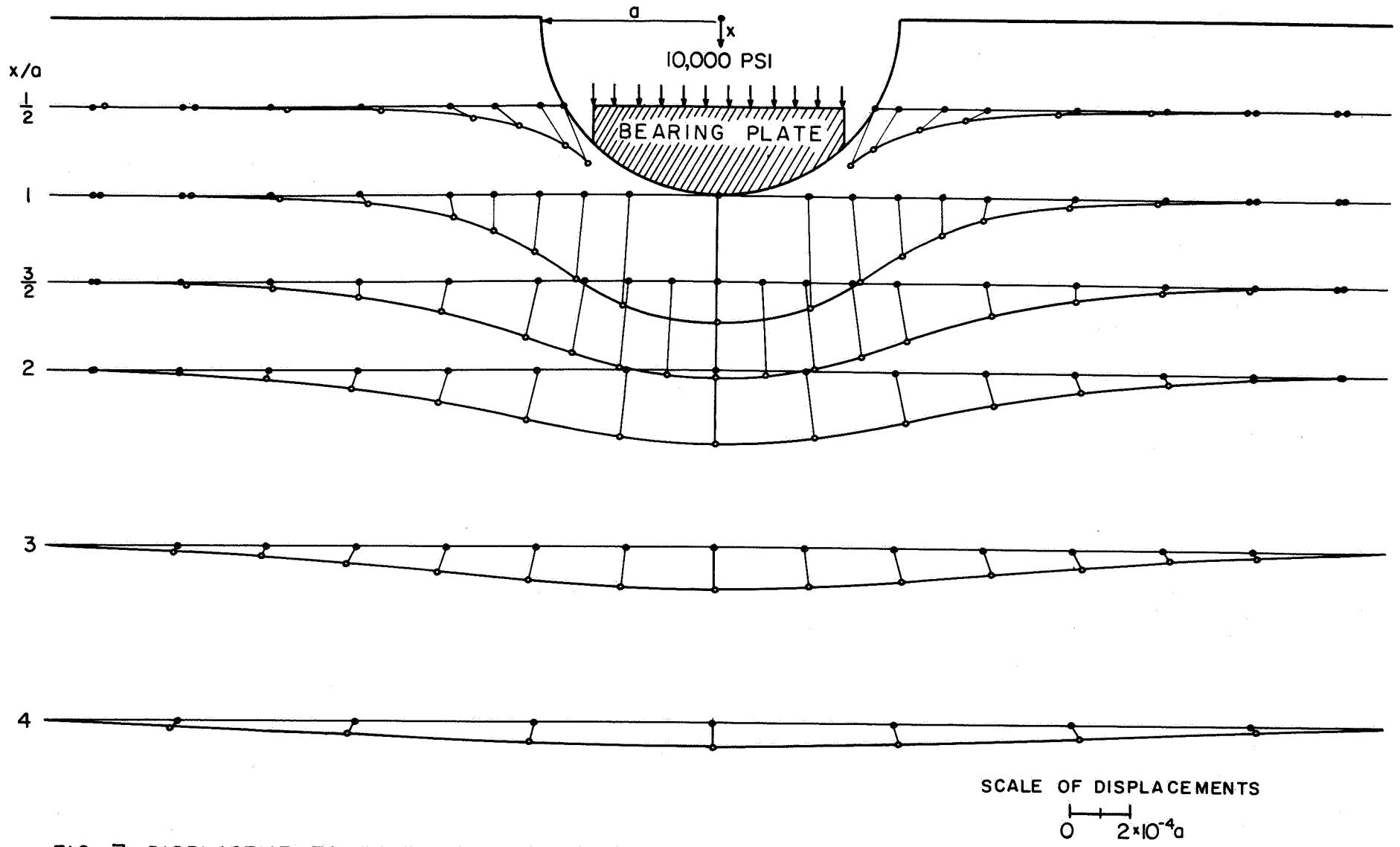

FIG. 7 DISPLACEMENTS OF ROCK UNDER 10,000 PSI LOAD BY BORE HOLE JACK.
ELASTIC MODULUS OF ROCK = 1.0×10^6 PSI.

decay of displacement with depth. The size of the test can be expressed by the volume of rock significantly stressed, say to a minimum of 1, 000 psi, and within which most, ca. 90%, of the displacement has occurred. At a plate pressure of 9, 000 psi this volume extends about 4.5 inches deep from the wall of the NX bore hole. Thus, the test may be considered as operating on an irregularly shaped rock domain roughly one foot in maximum extent. It is much larger than laboratory tests, and somewhat smaller than conventional plate bearing tests conducted in adits.

COMPARISON OF BORE HOLE JACK AND OTHER IN SITU TESTS

NX bore hole plate bearing tests were conducted in three underground test chambers where extensive in situ testing programs had been completed or were in progress. These were at the Tehachapi tunnel near Bakersfield (California Department of Water Resources); Dworshak dam near Orofino, Idaho (Walla Walla District, U. S. Corps of Engineers); and the Crestmore mine near Riverside, California (American Cement Co.). The quipment used in these tests included the NX bore hole plate bearing device, two Schaevitz servo indicators, a double acting 10, 000 psi hand pump, and Bourdon pressure gages, as depicted in figure 8.

At the test gallery of the Tehachapi project an adit to the discharge tunnel, the rock is a closely fractured diorite gneiss with seams of clay derived from the rock by hydrothermal alteration. Several hard, fresh pieces of core were obtained in drilling the NX holes for the bore hole plate bearing tests but the overall recovery was only fair. Four bore hole jack tests were conducted in two horizontal holes.

In situ tests included stress measurements, seismic measurements, and plate bearing tests. Four plate bearing tests were performed; and analyses were made of the data assuming both uniform and rotational deflec-

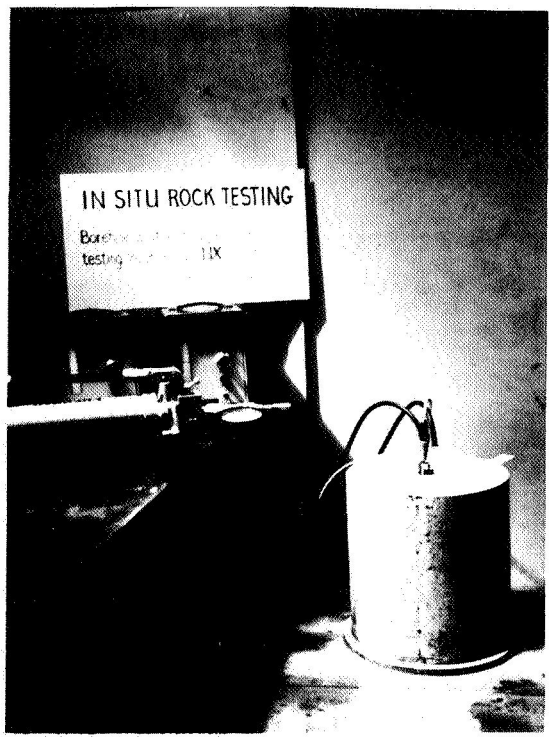

FIGURE 8. COMPLETE EQUIPMENT FOR NX BOREHOLE PLATE BEARING TEST. THE APPROXIMATE DIMENSIONS OF THE VOLUME OF ROCK UNDER TEST IN SITU IS INDICATED BY THE CONCRETE CYLINDER.

tions, as discussed by Kruse, et. al.[27], for similar tests at Oroville. Figure 9a presents a typical pressure versus diametral displacement curve for the bore hole jack tests at this location. The average value of E from plate bearing tests was 700, 000 psi; the average value of E from bore hole jack tests was 840, 000 psi in the same pressure range.

The Dworshak dam tests were conducted in a test gallery employed previously by Shannon and Wilson[28] for a comprehensive program of in situ rock tests. The rock at this site is a massive to moderately jointed epidote quartz-diorite gneiss. The in situ tests included plate bearing test, a chamber test, and seismic measurements.

There was great scatter in the results of plate bearing tests; the mean modulus of elasticity in plate bearing was 3. 4 million psi with individual results ranging from 500, 000 psi to 5 million psi. Fourteen bore hole jack tests were conducted in eight bore holes, three of which were water filled. The average modulus from these tests was 2. 1 million psi, with little scatter. A typical curve of pressure versus displacement for bore hole jack tests is shown in figure 9b.

An extensive program of in situ tests were completed by Heuzé and Goodman[29] at Crestmore mine, an underground room and pillar mine in massive, coarse, crystalline marble. In situ tests included flat jack measurements, plate bearing tests, and field seismic measurements. Bore hole jack tests were conducted in two horizontal bore holes at the site of the flat jack emplacements. The modulus of elasticity values computed from the load deformation curves on pressuring the flat jacks averaged 1. 8 million psi. The bore hole jacks gave an average value of 1. 5 million psi for E. A typical curve of plate pressure versus diametral displacement for the bore hole tests is given in figure 9c.

Table 5 is a summary and comparison of test results from the three areas.

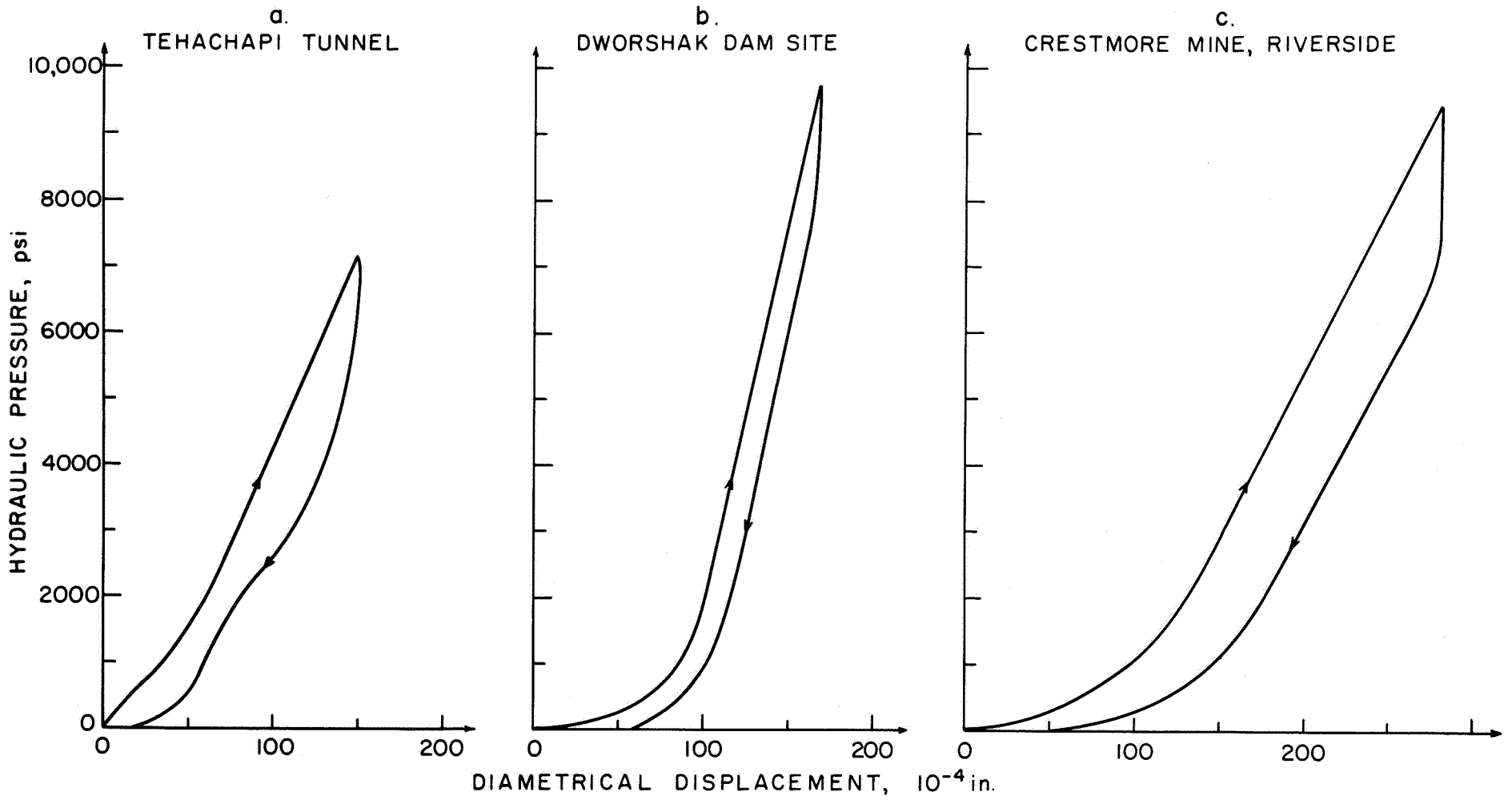

FIGURE 9. PRESSURE DEFORMATION CURVES FOR FIELD TESTS WITH Nx PLATE BEARING DEVICE.

TABLE 5

SUMMARY OF TEST RESULTS

Comparison of In Situ, Core, and Bore Hole Jack Tests

Site	Rock Type	Poisson's Ratio	Young's Modulus, 10^6 psi			
			Unconfined Compression (laboratory average)	Plate Bearing* (in situ)	Flat Jack* (in situ)	Bore Hole Jack* (in situ)
Tehachapi Tunnel	diorite gneiss; fractured and seamy	0.35	11.3	0.53 to 0.83		0.61 to 1.03
Dworshak Dam	granite gneiss; massive to moderately jointed	0.20	7.5	0.5 to 5.0		1.54 to 2.70
Crestmore Mine	marble; massive	0.25	6.9	1.74 to 2.72	1.79 to 2.98	1.35 to 1.70

*in the same pressure range 0-3,000 psi

At each of the sites, E was measured, additionally, in unconfined compression tests on NX core specimens in the laboratory. These values were, in all cases, considerably higher than the results of static tests in situ -- by a factor of 3 or more. This discrepancy between field and laboratory values is a common one in rock testing. Laboratory testing is usually conducted on solid samples which are not fully representative of the rock mass with its defects. The results of the bore hole jack tests were comparable to those of other in situ tests.

Bore hole jack tests are well suited to measurements of rock deformability at engineering sites. The tests are easier and less costly to conduct than plate bearing, flat jack, and other in situ techniques; thus many more measurements can be made. Furthermore, being conducted in drill holes, rock volumes remote from the surface can be tested. These facts allow one to establish the attributes of the rock mass quantitatively and qualitatively in every rock member reached by a work. The values obtained from these tests in three earth rock engineering cases discussed herein were comparable to values obtained by other more costly in situ techniques.

CONCLUSION

The following should be considered when rating the probes for lunar application:

1. What experience is there in its application?
2. How rugged is the probe? Can it be recovered after use? Are any fluids used?
3. How sensitive is it? What is the essential measuring device (volumetric gage, LVDT's, dial gage extensometer, etc.)?
4. Is the calibration very sensitive to pressure and extreme temperature variations?
5. What is the possibility of automatic recording and remote control? What is the nature of the output (digital, analog)? Can the operation be simu-

lated by digital techniques?

6. How cumbersome is the total measuring and monitoring instrumentation?

7. How easily can a rock deformability measurement be integrated into a complex bore hole experiment on the moon?

8. Would such a test endanger other experiments to be conducted in the same bore hole?

Answers to these questions are given in Table 6.

This study indicates that efforts should be directed towards the design and/or lunarization of a bore hole jack using LVDT's as monitoring units and providing automatic recording and transmission of digital output. The final probe could evolve from the instrument designed by Goodman, et. al., whose reliability in earth operation has been investigated here. As a further study, it is suggested that the use of narrow angle jacks be investigated for testing of soil and/or rubble strength characteristics.

ACKNOWLEDGEMENTS

The authors wish to thank the engineering agencies and personnel who generously offered their sites for field testing and furnished data from their own laboratory and in situ tests. We are particularly indebted to George Kruse and A. O'Neill of the California Department of Water Resources; Charles Monahan of Walla Walla District, U. S. Army Corps of Engineers and Frank Foster of the American Cement Company. We also acknowledge the help of Ann Finucane and Gloria Pelatowski. The NX bore hole plate bearing device was partially developed with the aid of a grant from the Pacific Gas and Electric Company. Studies at the Crestmore mine were supported by a grant from American Cement Company. This research was also partially supported by NASA Contract NSR 05-003-189. The authors are very grateful to Edward Wilson, Assistant Professor of Structural Engineering at the University of California, Berkeley, for allowing them to use his new prismatic space program.

TABLE 6

RATING OF ROCK DEFORMABILITY MEASURING DEVICES FOR LUNAR OPERATION.

TYPE	REFERENCE	PREVIOUS EXPERIENCE FOR DEFORMABILITY TEST	EASY TO OPERATE AND INTERPRET	INSENSITIVE TO SEVERE ENVIRONMENT	REMOTE OPERATION POSSIBILITY	EASY RETRIEVAL	EASILY INTEGRATED TO MULTIPURPOSE PROBE	POSSIBILITY OF USE IN SOILS	POSSIBILITY OF USE IN RUBBLE	CAN IT BE MINIATURIZED	OVERALL RATING
DILATOMETERS	1, 2	YES	NO	NO	YES	YES	YES	YES	NO	YES	B
	3	?	NO	NO	YES	YES	YES	YES	NO	YES	B
	4	YES	YES	NO	YES	YES	YES	YES	NO	YES ?	B
	5	YES	YES	NO ?	YES	YES	YES	YES	NO	YES	B
	6	YES	YES ?	NO ?	YES	YES	YES ?	YES	NO	YES ?	B
	7	YES	NO	NO	NO	YES	NO	YES	NO	NO	C
	8, 9	YES	NO	NO	NO	YES	NO	YES	NO	NO	C
BOREHOLE JACKS	19	YES	YES	YES ?	YES	YES	YES	YES	YES	YES ?	A
	10, 11	YES	NO	YES	NO	NOT ALWAYS	NO	NO	YES	NO	C
	20	YES	YES	YES ?	YES	YES	YES	YES	YES	YES ?	A
	12	NO	NO	YES ?	YES ?	YES	YES	NO	NO	YES ?	B
	13	YES	NO	YES	NO	NOT ALWAYS	NO	NO	NO	NO	C
	14	NO	NO	YES	NO	NO	NO	NO	NO	NO	C
	15	NO	NO	YES	NO	YES	NO	NO	NO	NO	C
BOREHOLE PENETRO-METERS	16	NO	YES IF SHALLOW	YES ?	NO	YES	NO	NO	NO	YES ?	C
	17	NO	NO	YES	YES ?	YES	YES	NO	NO	YES ?	C
	18	NO	NO	YES	YES ?	YES	YES	NO	NO	YES ?	C

RATING:
A COULD BE ADAPTED TO LUNAR MEASUREMENTS.
B ADAPTATION WOULD BE DIFFICULT, THUS UNLIKELY TO BE USED ON THE MOON.
C REJECT FOR LUNAR APPLICATION.

REFERENCES

1. Menard, L., "Mesures In-situ Des Propriétés Physiques des Sols," Annales des Ponts et Chaussées, No. 3, May-June 1957.

2. Menard, L., "Rules for the Calculation and Design of Foundation Elements on the Basis of Pressuremeter Investigations of the Ground," Translated by B. E. Hartmann, adjusted by J. B. Francq (distributed by Terrametrics), April 1966.

3. Geoprobe Instrument, literature by Testlab Corporation, 216 N. Clinton St., Chicago, Illinois, 60606, 1967.

4. Rocha, M., et.al., "Determination of the Deformability of Rock Masses Along Boreholes," Proceedings of 1st Congress of the International Society for Rock Mechanics, Vol. I, 1966, pp. 697-703.

5. Janod, A. and Mermin, P., "La Mesure des Caractéristiques des Roches en Place a l'Aide du Dilatomètre a Vérin.Cylindrique," Travaux, July 1954.

6. Comes, G., "Contribution a la Détermination Des Caracteristiques Mecaniques d'une Fondation Rocheuse," Travaux, November 1965.

7. Takano, M. and Shidomoto, Y., "Deformation Test on Mudstone Enclosed in a Foundation by Means of Tube Deformation," Proceedings of 1st Congress of the International Society for Rock Mechanics, Vol. I, 1966, pp. 761-764.

8. Kujundzic, B. and Stojakovic, M., "A Contribution of the Experimental Investigation of Changes of Mechanical Characteristics of Rock Massives as a Function of Depth," Transactions of the 8th Congress on Large Dams, Edinburgh, Great Britain, May 1964, pp. 1051-1067.

9. Kujundzic, B., "Experimental Research into Mechanical Characteristics of Rock Masses in Yugoslavia," International Journal of Rock Mechanics and Mining Sciences, England, Vol. 2, 1965, pp. 75-91.

10. Groupe de Travail du Comité National Francais, "Mesure des Modules de Déformation des Massifs Rocheux Dans Les Sondages," Proceedings 8th Congress on Large Dams, R. 16, Q. 28, May 1964, pp. 317-320.

11. Noel, G., "Mesure du Module d'Elasticité en Profondeur dans les Massifs Rocheux. Cellule de Mesure," De l'Institut Technique du Batiment et des Travaux Publics, No. 185, May 1963, pp. 533-540.

12. Talobre, J. A., "La Mesure In Situ des Propriétés Mécaniques des Roches et la Securité des Barrages de Grande Hauteur," R. 20, Q. 28, Proceedings 8th Congress on Large Dams, May 1964, pp. 397-399.

13. Martini, H. J., et.al., "Methods to Determine the Physical Properties of Rock," Proceedings 8 th Congress on Large Dams, May 1964, pp. 859-869.

14. Panek, L. A. and Stock, J. A., "Development of a Rock Stress Monitoring Station Based on Flat Slot of Measuring Existing Rock Stress," USBM Report of Investigation 6537, U. S. Bureau of Mines, 1964.

15. Jaeger, J. C. and Cook, N. G. W., "Theory and Application of Curved Jacks for Measurement of Stresses," International Conference on State of Stress in the Earth's Crust, Santa Monica, California, May 1963, Elsevier Press (ed. Judd), pp. 12-1.

16. Stears, J. H., "Evaluation of Penetrometer for Estimating Roof Bolt Anchorage," USBM Report of Investigation 6646, U. S. Bureau of Mines, 1965.

17. Hult, J., "On the Measurement of Stresses in Solids," Transactions of Chalmers University of Technology, Gothenburg, Sweeden, No. 280, 1963.

18. Dryselius, G., "Konstricktion au Matcel for Beigtrycksstudier" (Design of a Measuring Cell for the Study of Rock Pressure), IVA Ingeniorsvetenskapsakademiens Meddelande, 142, Stockholm, 1965, pp. 135-144.

19. Goodman, R. E., "Research In Geological Engineering at the University of California, Berkeley," Proceedings of 4th Annual Symposium on Engineering Geology and Soils Engineering, Moscow, Idaho, Idaho Department of Highways, 1966, pp. 155-165.

20. Absi, E. and Seguin, M., "Le Nouveau Géoextensomètre," Supplement to Annales de L'Institut Technique du Batiment et des Travaux Publics, No. 235-236, July-August 1967, pp. 1151-1158.

21. Ladanyi, B., "Evaluation of Pressuremeter Tests in Granular Soils," Proceedings of 2nd Panamerican Conference on Soil Mechanics and Foundation Engineering, Vol. 1, 1963, pp. 1-20.

22. Ladanyi, B., "Etude Théorique et Expérimentale de l'Expansion dans un Sol Pulvérulent d'une Cavité Présentant une Symétrie Sphérique ou Cylindrique, Annales des Travaux Publics de Belgique, Bruxelles, Vol. 2 and 4, 1961.

23. Gibson, R. E. and Anderson, W. F., "In-situ Measurement of Soil Properties with the Pressuremeter," Civil Engineering and Public Works Review, London, May 1961.

24. Groupe de Travail du Comité National Francais, "Mesure des Modules de Deformation des Massifs Rocheux Dans les Sondages," Proceedings 8th Congress on Large Dams, R. 16, Q. 28, May 1964, pp. 320-323.

25. Jaeger, J. C., Elasticity, Fracture and Flow, Methuen and Co., London, 2nd ed., 1962.

26. Wilson, E. L., "Stress Analysis of Prismatic Solids," SESM Report, Dept. Civil Engineering, University of California, Berkeley (in press) 1967.

27. Stropponi, E. W. and Kruse, G. H., "Discussion of 'Foundation Modulus Tests for Karadj Arch Dam' " by Waldorf, et al., Journal Soil Mechanics and Foundation Division, Proceedings, ASCE, Vol. 90, No. SM 2, March 1964, pp. 191-205.

28. Shannon and Wilson, Inc., "In Situ Rock Tests for Dworshak Dam Site," January 25, 1965.

29. Heuzé, F. E. and Goodman, R. E., "Mechanical Properties and In Situ Behavior of the Chino Limestone, Crestmore Mine, Riverside, California," Proceedings 9th Symposium on Rock Mechanics, AIME, April 1967 (in press).

30. Suzuki, K., "Fundamental study of rock stress measurements by borehole deformation method," Proceedings 1st Congress of Int'l Soc. Rock Mechanics, Vol. II, pp. 35-39.

31. Agarrval, R., "Sensitivity analysis of borehole deformation measurements of in situ stress determination when affected by borehole excentricity," Proceedings 9th Symposium on Rock Mechanics, Golden, Colorado, April 1967.

APPENDIX

SOLUTION OF UNIAXIAL STRESS PROBLEM BY COMPLEX VARIABLE METHOD

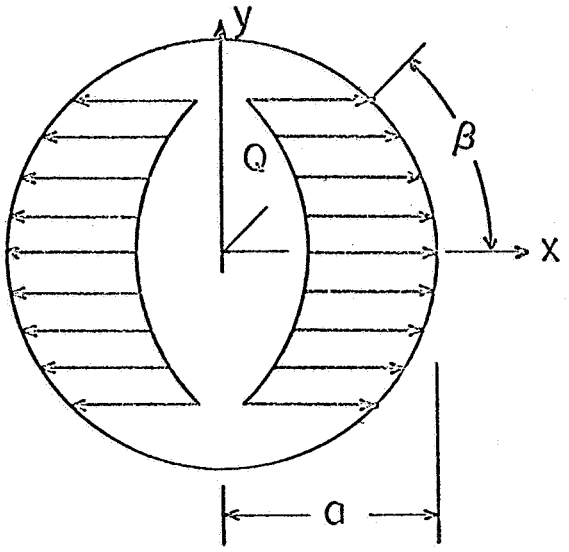

Boundary condition at $r = a$, $\sigma_y = 0$, and $\tau_{xy} = 0$

$$\sigma_x = \begin{cases} Q & -\beta < \theta < \beta \quad , \qquad \pi - \beta < \theta < \beta + \pi \\ 0 & \beta < \theta < \pi - \beta \quad , \qquad \pi + \beta < \theta < 2\pi - \beta \end{cases} \tag{1}$$

At θ from x - axis ($Q = 2p$):

$$\begin{aligned} \sigma_r &= p + p\cos 2\theta \\ \sigma_\theta &= p - p\cos 2\theta \\ \tau_{r\theta} &= -p\sin 2\theta \end{aligned} \tag{2}$$

The problem can be conveniently decomposed into two more simple problems, A and B. Each problem will be solved separately, and the results are added. The displacement relations and the stress relations are expressed in complex forms.

A. UNIFORM STRESS OVER TWO SYMMETRICAL PORTIONS OF THE CIRCULAR BOREHOLE*

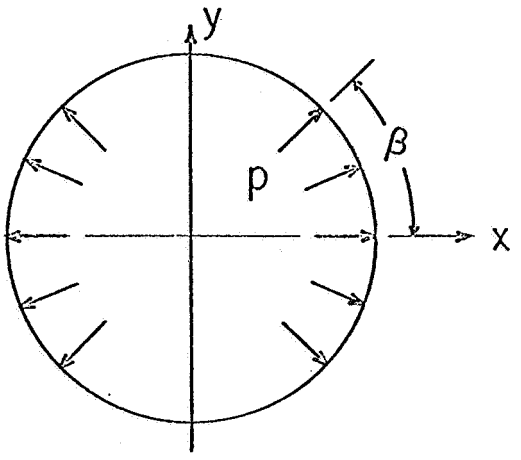

Boundary conditions at r = a

$$\tau_{r\theta} = 0 \tag{3}$$

$$\sigma_r = \begin{cases} p & -\beta < \theta < \beta \quad , \quad \pi - \beta < \theta < \pi + \beta \\ 0 & \beta < \theta < \pi - \beta \quad , \quad \pi + \beta < \theta < 2\pi - \beta \end{cases} \tag{4}$$

$$\sigma_r - i\tau_{r\theta} = \sum_{n=-\infty}^{\infty} An\ e^{in\theta} \tag{5}$$

where

$$An = \frac{1}{2\pi} \int_0^{2\pi} (\sigma_r - i\tau_{r\theta})\ e^{-in\theta}\ d\theta \tag{6}$$

$$\sigma_r - i\tau_{r\theta} = \phi'(z) + \overline{\phi'(z)} - [\, z\,\phi''(z) + \chi''(z)\,]\ e^{2i\theta} \tag{7}$$

---

*This problem was first solved by Jaeger and Cook in State of Stress in the Earth's Crust (W. R. Judd, ed.), Elsevier, 1964, p. 381-396.

$$\phi'(z) = \sum_{n=0}^{\infty} a_n z^{-n}$$

$$\chi''(z) = \sum_{n=0}^{\infty} b_n z^{-n} \qquad (8)$$

$$a_0 = b_0 = 0$$

$$\xi a_1 + \overline{b_1} = 0 \qquad (9)$$

Solve for a_n and b_n:

$$\phi'(z) = \sum_{n=0}^{\infty} a_n z^{-n} = \sum_{m=1}^{\infty} \frac{p a^{2m}}{m \pi} \sin 2m\beta \; z^{-2m} \qquad (10)$$

$$\chi''(z) = \sum_{n=0}^{\infty} b_n z^{-n} = -\frac{2\beta p}{\pi} a^2 z^{-2} + \sum_{m=1}^{\infty} \frac{2 p a^{2(m+1)}}{\pi} \sin 2m\beta \; z^{-2(m+1)} \qquad (11)$$

Determination of Displacement:

$$2G(u_r + i u_\theta) = [\xi \phi(z) - z\overline{\phi'(z)} - \overline{\chi(z)}] e^{-i\theta} \qquad (12)$$

$$2G u_r = \text{Real (R.H.S.)} = -\frac{2\beta p \rho a}{\pi} + \sum_{m=1}^{\infty} \frac{\xi p \rho^{(2m-1)}}{m(1-2m)} a \sin 2m\beta \cos 2m\theta$$

$$- \sum_{m=1}^{\infty} \frac{p \rho^{(2m-1)}}{m \pi} a \sin 2m\beta \cos 2m\theta$$

$$+ 2 \sum_{m=1}^{\infty} \frac{p \rho^{2(m+1)}}{\pi (2m+1)} a \sin 2m\beta \cos 2m\theta \qquad (13)$$

$$\rho = 1 = \frac{r}{a}$$

$$2 G u_r \frac{\pi}{p a} = - 2 \beta - \sum_{m=1}^{\infty} \frac{1}{m} \left[\frac{\xi}{2 m - 1} + \frac{1}{2 m + 1} \right] \sin 2 m \beta \cos 2 m \theta \qquad (14)$$

Stress Determination:

$$\sigma_\theta + \sigma_r = 4 \text{ Real } [\phi' (z)] \qquad (15)$$

$$\sigma_\theta - \sigma_r + 2 i \tau_{r\theta} = 2 [\bar{z} \phi'' (z) \div \chi'' (z)] e^{2i\theta} \qquad (16)$$

$$\sigma_\theta \frac{\pi}{p} = - 2 \beta \rho^2 + 2 \sum_{m=1}^{\infty} \frac{1}{m} \rho^{2m} (m \rho^2 - m + 1) \sin 2 m \beta \cos 2 m \theta \qquad (17)$$

$$\sigma_r \frac{\pi}{p} = 2 \beta \rho^2 + 2 \sum_{m=1}^{\infty} \frac{1}{m} \rho^{2m} (m \div 1 - m \rho^2) \sin 2 m \beta \cos 2 m \theta \qquad (18)$$

$$\tau_{r\theta} \frac{\pi}{p} = 2 (1 - \rho^2) \sum_{m=1}^{\infty} \rho^{2m} \sin 2 m \theta \sin 2 m \beta \qquad (19)$$

B. THE EXPONENTIAL BOUNDARY CONDITION PROBLEM: $\sigma_r - i\,\tau_{r\theta} = p\,e^{2i\theta}$ *

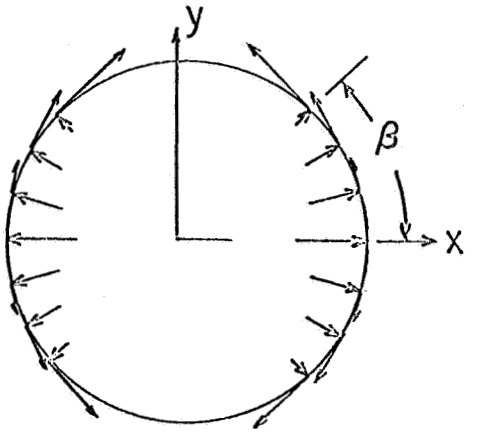

Boundary Condition at r = a

$$\sigma_r = \begin{cases} p\cos 2\theta & -\beta < \theta < \beta \\ 0 & \beta < \theta < \pi - \beta \end{cases}$$

$$\tau_{r\theta} = \begin{cases} -p\sin 2\theta & \pi - \beta < \theta < \pi + \beta \\ 0 & \pi + \beta < \theta < 2\pi - \beta \end{cases} \qquad (20)$$

With boundary conditions (5) and (7) where An is defined by (6), the Fourier series representation of boundary conditions:

$$\sigma_r - i\,\tau_{r\theta} = \begin{cases} p\,(\cos 2\theta + i\sin 2\theta) = p\,e^{2i\theta}, & -\beta < \theta < \beta, \quad \pi - \beta < \theta < \pi + \beta \\ 0, & \beta < \theta < \pi - \beta, \quad \pi + \beta < \theta < 2\pi - \beta. \end{cases} \qquad (21)$$

*To the authors' knowledge this problem has not been solved before.

Using (9) and computing for a_n and b_n:

$$\phi'(z) = \sum_{n=0}^{\infty} a_n z^{-n} = \frac{2 p \beta}{\pi} a^2 z^{-2} + \sum_{m=2}^{\infty} \frac{p a^{2m}}{\pi(m-1)} \sin 2(m-1) \beta z^{-2m} \tag{22}$$

$$\chi''(z) = \sum_{n=0}^{\infty} b_n z^{-n} = -\frac{p a^2}{\pi} \sin 2\beta z^{-2} - \frac{p a^4}{2\pi} \sin 4\beta z^{-4} + \frac{6 p \beta}{\pi} a^4 z^{-4}$$

$$+ \sum_{m=2}^{\infty} \frac{(2m+1)}{\pi(m-1)} p a^{2(m+1)} \sin 2(m-1) \beta z^{-2(m+1)}$$

$$- \sum_{m=2}^{\infty} \frac{p a^{2(m+1)}}{\pi(m+1)} \sin 2(m+1) \beta z^{-2(m+1)} \tag{23}$$

Calculation of Displacements:

Using (12) at $\rho = 1$

$$2 G u_r \frac{\pi}{p a} = -2 \xi \beta \cos 2\theta - \sum_{m=1}^{\infty} \frac{1}{m} \left[\frac{\xi}{2m+1} \cos 2(m+1)\theta \right.$$

$$\left. + \frac{1}{2m-1} \cos 2(m-1)\theta \right] \sin 2m\beta \tag{24}$$

Calculation of Stresses:

Using (15) and (16)

$$\sigma_\theta \frac{\pi}{p} = 6 \beta \rho^4 \cos 2\theta - \sum_{m=2}^{\infty} \frac{2 \rho^{2m}}{m-1} \left[2m - 2 - (2m+1) \rho^2 \right] \sin 2(m-1) \beta \cos 2m\theta$$

$$- \sum_{m=0}^{\infty} \frac{\rho^{2(m+1)}}{m+1} \sin 2(m+1) \beta \cos 2m\theta \tag{25}$$

$$\sigma_r \frac{\pi}{p} = 8 \beta \rho^2 \cos 2\theta + \sum_{m=2}^{\infty} \frac{\rho^{2m}}{(m-1)} [2 + 2m - (2m+1)\rho^2] \sin 2(m-1)\beta \cos 2m\theta$$

$$+ \sum_{m=0}^{\infty} \frac{\rho^{2(m+1)}}{(m+1)} \sin 2(m+1)\beta \cos 2m\theta \qquad (26)$$

$$\tau_{r\theta} \frac{\pi}{p} = 2 \beta \rho^2 (2 - 3\rho^2) \sin 2\theta$$

$$+ \sum_{m=2}^{\infty} \frac{\rho^{2m}}{(m-1)} [2m - (2m+1)\rho^2] \sin 2(m-1)\beta \sin 2m\theta$$

$$+ \sum_{m=0}^{\infty} \frac{\rho^{2(m+1)}}{(m+1)} \sin 2(m+1)\beta \sin 2m\theta \qquad (27)$$

C. NET RESULTS -- Obtained by Summing Solutions of A and B.

Net Radial Displacement

Add (14) and (24) to obtain the net radial displacement relation:

$$2 G u_r \frac{\pi}{p a} = -2\beta(1 + \xi \cos 2\theta) - \sum_{m=1}^{\infty} \frac{1}{m} \sin 2m\beta \left[\frac{\xi}{2m+1} \cos 2(m+1)\theta + \left(\frac{\xi}{2m-1} + \frac{1}{2m+1}\right) \cos 2m\theta + \frac{1}{2m-1} \cos 2(m-1)\theta \right] \quad (28)$$

At $\theta = 0$, radial displacements is maximum.

$$2 G u_{rmax} \frac{\pi}{p a} = -2\beta(1 + \xi) - \sum_{m=1}^{\infty} \frac{4(\xi+1)}{(2m+1)(2m-1)} \sin 2m\beta \quad (29)$$

For the application of the results to the calculation of modulus of deformability, it is necessary to obtain a relation containing the integrated value of displacement.

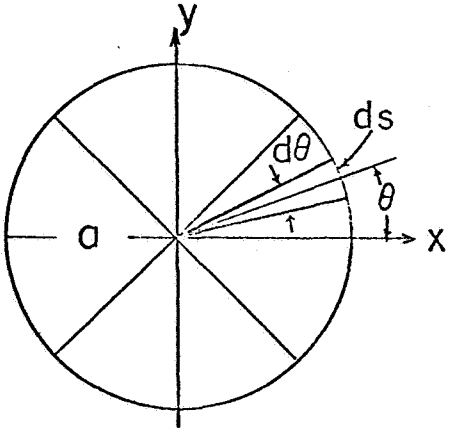

$$dy = ds \cos\theta = a \cos\theta \, d\theta$$

$$\left[2 G \bar{u}_r \frac{\pi}{p a}\right] a \sin\beta = \int_0^{\beta} [\text{R.H.S. (28)}] \, a \cos\theta \, d\theta \quad (30)$$

Replacing $\xi = 3 - 4\nu$ in the result gives:

$$\left[2 G \bar{u}_r \frac{\pi}{p a} \right] \sin\beta = -2\beta \left[\frac{5 - 4\nu}{2} \sin\beta + \frac{3 - 4\nu}{6} \sin 3\beta \right]$$

$$- \sum_{m=1}^{\infty} \frac{1}{2m} \sin 2m\beta \left[\frac{3 - 4\nu}{2m + 1} \left[\frac{\sin (2m + 1)\beta}{2m + 1} + \frac{\sin (2m + 3)\beta}{2m + 3} \right] \right.$$

$$+ \left[\frac{3 - 4\nu}{2m - 1} + \frac{1}{2m + 1} \right] \left[\frac{\sin (2m - 1)\beta}{2m - 1} + \frac{\sin (2m + 1)\beta}{2m + 1} \right]$$

$$\left. + \frac{1}{2m - 1} \left[\frac{\sin (2m - 3)\beta}{2m - 3} + \frac{\sin (2m - 1)\beta}{2m - 1} \right] \right] \qquad (31)$$

Net σ_θ

Add (17) and (25) and rearrange the terms.

$$\sigma_\theta \frac{\pi}{p} = -2\beta\rho^2 + 6\beta\rho^4 \cos 2\theta + \sum_{m=0}^{\infty} \frac{\rho^{2(m+1)}}{m + 1} \sin 2(m + 1)\beta$$

$$\left[\cos 2m\theta + \left[(m + 1)\rho^2 - m \right] \cos 2(m + 1)\theta \right.$$

$$\left. + \left[(2m + 3)\rho^2 - 2m - 2 \right] \cos 2(m + 2)\theta \right] \qquad (32)$$

At $\theta = \pi/2$, $\rho = 1$ σ_θ is maximum. Replacing

$$\cos 2m\theta = \begin{cases} +1 & m = 0, 2, 4, \ldots \\ -1 & m = 1, 3, 5, \ldots \end{cases}$$

into (32)

$$\sigma_\theta \, \pi/p = -8\beta \qquad (33)$$

For $\beta = \pi/4$ ($Q = 2p$), $\sigma_\theta = -Q$ (34)

This result checks with finite element analysis.

At $\theta = 0, \quad \rho = 1.$

$$\sigma_\theta \frac{\pi}{p} = 4\beta + \sum_{m=0}^{\infty} \frac{3}{m+1} \sin (m+1)\, 2\beta$$

For $\beta = \frac{\pi}{4}$

$$\sigma_\theta \frac{\pi}{p} = \pi + 3 \text{ Arc tan } 1 = \pi + \frac{3\pi}{4} \text{ then } \sigma_\theta = 1.75\, p = 0.875\, Q$$

Net σ_r

Add (18) and (26) and rearrange the terms.

$$\sigma_r \frac{\pi}{p} = 2\beta\rho^2 [\, 1 + (4 - 3\rho^2) \cos 2\theta \,] + \sum_{m=0}^{\infty} \frac{\rho^{2(m+1)}}{m+1} \sin 2 (m+1)\beta$$

$$\left[\cos 2m\theta + [\, m+2-(m+1)\rho^2 \,] \cos 2(m+1)\theta \right.$$

$$\left. + [\, 2m+4-(2m+3)\rho^2 \,] \cos 2(m+2)\theta \right] \qquad (35)$$

Net $\tau_{r\theta}$

Add (19) and (27) and rearrange the terms.

$$\tau_{r\theta} \frac{\pi}{p} = 2\beta\rho^2 (2 - 3\rho^2) \sin 2\theta + \sum_{m=0}^{\infty} \rho^{2(m+1)} \sin 2 (m+1)\beta$$

$$\left[\frac{1}{m+1} \sin 2m\theta + 2(1-\rho^2) \sin 2(m+1)\theta \right.$$

$$\left. + \frac{1}{m+1} [\, 2m+4-(2m+5)\rho^2 \,] \sin 2(m+2)\theta \right] \qquad (36)$$

Equation (31) is used in the calculation of the modulus of deformation in terms of applied pressures and corresponding deformations. Using $Q = 2p$, $\bar{u}_d = 2\bar{u}_r$, $d = 2a$, and $G = E/(2(1+\nu))$, (31) can be rewritten as:

$$E = \frac{1}{\sin\beta} \frac{(1+\nu)\,d}{2\pi} \frac{Q}{\bar{u}_d} \left[\text{R. H. S.}\right]$$

$$E = K(\nu,\beta) \frac{Q\,d}{\bar{u}_d} \qquad (37)$$

Values of $K(\nu,\beta)$ are expressed in Table 2 for different values of ν and β. Q is the pressure actually applied to the rock (see 37). The variation of $K(\nu,\beta)$ with respect to β is shown in Figure 2 for values of $\nu = 0.25$, 0.40, and 0.10. It is observed that K has a maximum value at $\beta = 45^{\circ}$, the case of the NX bore hole uniaxial jack.

NOTE: R. H. S. signifies the terms to the right of the equal sign in Equation (31).